Transverse currents in triplet Josephson junction with spin-orbit coupling

Huan Zhang, K. S. Chan, Zijing Lin, and J. Wang

Phys. Rev. B **85**, 024501 — Published 3 January 2012
DOI: 10.1103/PhysRevB.85.024501

Transverse currents in triplet Josephson junction with spin-orbit coupling

Huan Zhang,[1,2,3] K S Chan,[1,*] Zijing Lin,[2,†] and J Wang[4]

[1] *Department of Physics and Materials Science, City University of Hong Kong, Hong Kong, China*
[2] *Department of Physics, University of Science and Technology of China, Hefei, 230026, China*
[3] *USTC-CityU Joint Advanced Research Centre, Suzhou, 215123, China*
[4] *Department of Physics, Southeast University, Nanjing, 210096, China*

(Dated: December 20, 2011)

We investigate theoretically the equilibrium transverse charge and spin currents flowing in a hybrid Josephson junction composed of two triplet p-wave superconductors and a Rashba spin-orbit coupling (RSOC) layer in between. Through a symmetry analysis, we show that the transverse currents originate from the breaking of mirror symmetries due to the misalignment of $\boldsymbol{d}$-vectors in the two triplet superconductor leads. Besides, the mirror symmetries strongly constrain the dependence of the transverse currents on both the absolute and relative angles of the $\boldsymbol{d}$-vectors. The symmetry analysis is confirmed by the numerical calculations based on the lattice Matsubara Green's function method. The dependence of the transverse currents on the RSOC strength as well as the middle layer length is also addressed. These findings shed new light on the equilibrium spintronics device design and are useful for identifying the order parameter symmetries of p-wave superconductors.

PACS numbers: 74.50.+r, 74.20.Rp, 71.70.Ej, 74.25.F-, 72.25.-b, 85.25.Cp

I. INTRODUCTION

Transverse transports, such as charge and spin Hall currents, have been intensively studied in the multiple terminal semiconductors and metals. When a Zeeman field is applied on a cross section, a transverse charge voltage/current can be induced by a longitudinal current, which is the famous Hall effect (HE)[1]. Another remarkable phenomenon, either intrinsic or extrinsic spin Hall effect (SHE)[2–6], has been discussed extensively in literatures. A spin Hall effect is referred to as a transverse pure spin current generated by a longitudinal charge current in a spin-orbit coupling media. To realize HE or SHE, however, a longitudinal voltage bias or spin injection is needed, i.e., both HE and SHE work at a nonequilibrium state. Naturally, a question rises: can we observe equilibrium transverse currents in some systems driven by other than the electric field or spin injection?

Among the equilibrium systems, stationary Josephson junction[7,8] is a promising choice. Actually, Josephson junctions with Zeeman field and/or SOC have been intensively investigated and many novel phenomena[9–16] have been reported, such as Josephson π-junction[9–11] and anomalous Josephson effect[12,13]. However, those studies had only concentrated on the longitudinal transport properties. Recently, some efforts were dedicated to the transverse transport behaviors. Mal'shukov *el at*[17] predicted a out-of-plane spin Hall polarization at the lateral edges of Josephson junction with a SOC in between. In their later study[18], an inverse SHE was further predicted when an inhomogeneous Zeeman field is applied on the system in addition to the SOC. However, no explicit transverse charge/spin current was found in their system where only the singlet s-wave superconductor was considered in the superconducting leads.

Compared with the singlet s-wave superconductor, the triplet superconductor (TS), demonstrated in numerous experiments[19,20], has attracted increasing interest in the field of superconducting junctions and many peculiar transport properties have been predicted in the TS junctions[21–29]. Those novel properties, such as the spin current[24–27] and accumulation[27–29], are due to the subtle spin structure of the TS pair potential, characterized by the $\boldsymbol{d}$-vector, along which the spin projection of triplet pair is zero[30]. Therefore, the TS junction with RSOC ignites the new possibility of generating the transverse currents in the equilibrium systems.

In this work, we study a p_x-wave TS Josephson junction with a Rashba SOC (RSOC) layer in between and focus on the transverse charge and spin currents. Based on a symmetry analysis, it is found that both equilibrium transverse charge and spin currents are forbidden by some mirror symmetries existing at certain special orientations of two $\boldsymbol{d}$-vectors in the TS leads. Apart from those special orientations, the transverse currents are possible. The symmetry analysis are numerically confirmed with the help of lattice Green's function method. The effects of the RSOC strength and the length of RSOC layer are also numerically studied.

This paper is organized in the following way. In Sec. II, we introduce the model and present the formulae to calculate transverse charge current and spin current. In Sec. III, we employ several mirror transformations to illustrate the origin of transverse currents. In Sec. IV, we discuss the numerical results of the paper. A conclusion is drawn in the last section.

II. MODEL AND FORMALISM

Let us consider a schematic p_x-wave TS/RSOC/p_x-wave TS (p_x/RSOC/p_x) junction in a square lattice, as shown in Fig. 1. The length of the RSOC layer is set as La and the width of junction is Wa, where a is the lattice constant. A lattice site is denoted by a vector $\boldsymbol{r} = l\boldsymbol{a}_x + w\boldsymbol{a}_y$, where $\boldsymbol{a}_x$ and $\boldsymbol{a}_y$ are the basis vectors in the x and y directions, respectively. The RSOC layer bridges two TS leads from $l = -L/2$ to $l = L/2$. Both $\boldsymbol{d}$-vectors in the left and right TS lead, $\boldsymbol{d}_L$ and $\boldsymbol{d}_R$, are in the yz plane, parameterized by an azimuthal angle θ_L and θ_R with respect to the z axis. $\theta_{L,R}$ varies from 0 to 2π and $-\theta_{L,R}$ is equivalent to $2\pi - \theta_{L,R}$. Throughout this paper, we assume the periodic boundary condition in the y direction and thus the transverse momentum k_y is a good quantum number.

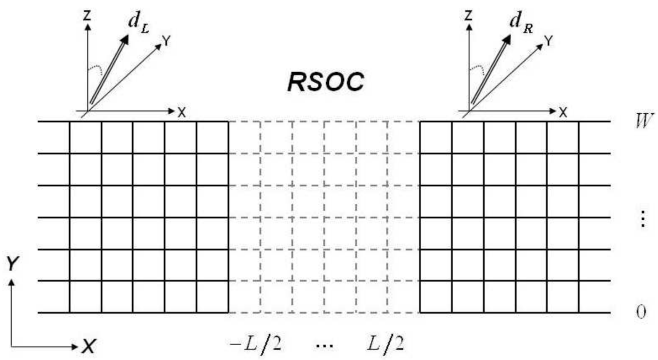

FIG. 1: Schematic of the p_x/RSOC/p_x junction. The lattice is in the xy plane. The two TS are connected through a RSOC layer residing from $l = -L/2$ to $l = L/2$. $\boldsymbol{d}_{L,R}$ in the yz plane has an angle $\theta_{L,R}$ with the z axis. The absolute(relative) angle is defined as $\theta_a(\theta_b)$= $(\theta_L \pm \theta_R)/2$.

The following mean-field Hamiltonian in a lattice version is employed to describe the system

$$H = -t \sum_{l\sigma,k_y} c^{\dagger}_{l\sigma,k_y} c_{l\pm 1\sigma,k_y} + \sum_{l\sigma,k_y} \left[\varepsilon_{l,k_y} - \mu\right] c^{\dagger}_{l\sigma,k_y} c_{l\sigma,k_y} + \sum_{l\sigma,k_y} \sum_{l'\sigma'} h_{l\sigma,l'\sigma'} c^{\dagger}_{l\sigma,k_y} c_{l'\sigma',k_y} - \sum_{l\sigma,k_y} \sum_{l'\sigma'} \left[\Delta_{l\sigma,l'\sigma'} c^{\dagger}_{l\sigma,k_y} c^{\dagger}_{l'\sigma',k_y} + h.c.\right], \quad (1)$$

where $c^{\dagger}_{l\sigma,k_y}(c_{l\sigma,k_y})$ is the creation (annihilation) operator of an electron in column l with spin σ (= $\uparrow$ or $\downarrow$) and transverse momentum k_y. The on-site energy ε_{l,k_y} has the form $4t - 2t\cos(k_y a) + V_l$, where V_l is the on-site potential. V_l except at interface is set to be zero (i.e. $V_l = 0$, for $l \neq -L/2 - 1$ or $L/2 + 1$), while V_l at the interface (i.e. $l = -L/2 - 1$ and $L/2 + 1$) is set to be V_B to simulate a barrier. The Fermi energy μ and the nearest-neighbor hopping integral t are assumed to be the same in the TS leads and the RSOC layer. Throughout this paper, we fix $\mu = 2t$. The Rashba spin-orbit coupling $h_{l\sigma,l'\sigma'}$ and the pair potential $\Delta_{l\sigma,l'\sigma'}$ in the spin space respectively reads

$$\breve{h}_{ll'} = t_{so}\sigma_x \sin(k_y a)\,\delta_{l,l'} \pm i t_{so}\sigma_y \delta_{l\pm 1,l'}/2, \quad (2)$$

$$\breve{\Delta}_{ll'} = \Delta(T)\, e^{i\varphi} \times \left(\pm \boldsymbol{d}\cdot\hat{\boldsymbol{\sigma}}\sigma_y \delta_{l\pm 1,l'}/2\right), \quad (3)$$

where t_{so} denotes the RSOC strength, φ is the superconducting phase, and $\Delta(T)$ is the BCS gap function. $\boldsymbol{d}$ is a unit vector. σ_i with $i = x, y, z$ are the Pauli matrices. For simplicity, the pair potentials in the two TS leads are set to be equal in amplitude $\Delta(T = 0) = \Delta$.

In the RSOC region, the charge operator in column l with transverse momentum k_y is defined as

$$\hat{\rho}_{l,k_y} = e\tilde{c}^{\dagger}_{l,k_y}\sigma_0 \tilde{c}_{l,k_y}, \quad (4)$$

where $\tilde{c}_{l,k_y} = \left[c_{l\uparrow,k_y}(\bar{t}), c_{l\downarrow,k_y}(\bar{t})\right]^T$, and σ_0 is the unit matrix, and $\bar{t}$ is the time. By using the Heisenberg equation $i\hbar\partial_{\bar{t}}\hat{\rho} = [\hat{\rho}, H]$, the operator of transverse charge current is found. Then we can construct the the Matsubara Green's function for calculating the transverse charge current i_y in column l as follows

$$i_y(l) = \frac{v_f}{W}\sum_{k_y}\left[\sin(k_y a)\,\rho(l,k_y) + \cos(k_y a)\,\rho_x(l,k_y)\right], \quad (5)$$

$$\rho(l,k_y) = \frac{e}{\beta}\sum_n \mathrm{Tr}\begin{bmatrix}\sigma_0 & 0\\ 0 & \sigma_0\end{bmatrix}\check{\mathcal{G}}_{\omega_n}(l,l;k_y), \quad (6)$$

$$\rho_x(l,k_y) = \frac{e t_{so}}{2\beta t}\sum_n \mathrm{Tr}\begin{bmatrix}\sigma_x & 0\\ 0 & \sigma_x^*\end{bmatrix}\check{\mathcal{G}}_{\omega_n}(l,l;k_y). \quad (7)$$

where $\rho(l,k_y)$ is the charge originating only from the hopping energy t while $\rho_x(l,k_y)$ is due to the nonzero RSOC t_{so} and sharing the similar form as the x-polarized spin[32]; $v_f = 2at/\hbar$ is the Fermi velocity in the y direction at $\mu = 2t$, $1/\beta = k_B T$, and $\omega_n = (2n+1)k_B T$ with k_B the Boltzmanm constant; $\check{\mathcal{G}}_{\omega_n}(l,l;k_y)$ is the Matsubara Green's function for mode k_y in the Nambu and spin spaces. The Matsubara Green's function is worked out by the Dyson equation $\check{\mathcal{G}}_{\omega_n} = \left[i\omega_n - H_c - \Sigma^L - \Sigma^R\right]^{-1}$, where H_c is the interaction matrix of the lattice sites in the same column. Σ^L and Σ^R are the self-energies of the left and right TS leads, respectively, which can be obtained by the recursive Green's function method[31].

By defining the spin operator as

$$\hat{\boldsymbol{s}}_{l,k_y} = (\hbar/2)\,\tilde{c}^{\dagger}_{l,k_y}\hat{\boldsymbol{\sigma}}\tilde{c}_{l,k_y} \quad (8)$$

and following the same procedure as deriving i_y, we can also obtain the out-of-plane transverse spin current j^z_y, which is given by

$$j^z_y(l) = \frac{v_f}{W}\sum_{k_y}\sin(k_y a)\, s_z(l,k_y), \quad (9)$$

$$s_z(l,k_y) = \frac{\hbar t_{so}}{4\beta t}\sum_n \mathrm{Tr}\begin{bmatrix}\sigma_z & 0\\ 0 & \sigma_z^*\end{bmatrix}\check{\mathcal{G}}_{\omega_n}(l,l;k_y), \quad (10)$$

where $s_z(l, k_y)$ denotes the z-polarized spin in column l with mode k_y.

The notation of the transverse current $I_y(J_y^z)$ used in Sec. IV is the average of $i_y(j_y^z)$ from column $l = -L/2-1$ to $L/2+1$. Note that the transverse currents should decay into the two TS leads and the contribution there is not considered. In numerical calculations, all currents have been divided by the lattice constant a, thus they actually have the unit of 'current density'. However, we still use the term 'current' for simplicity. Moreover, a large W is chosen to ensure the results independent of the width.

III. SYMMETRY ANALYSIS

Before presenting the numerical results of the transverse currents, it is instructive to analyze our junction based on certain symmetry arguments, because any current flowing in the system is coming from some broken symmetry, e.g., the supercurrent originates from the broken longitudinal mirror symmetry. Similarly, the transverse currents should also stem from certain broken symmetries, and the symmetry analysis can thus offer a deep insight into their origins. In what follows, the mirror symmetries are found to exist at some special $\theta_{L,R}$, where the transverse currents are forbidden.

Let us start with the mirror transformation perpendicular to the xz plane, denoted by the operator M_y. It transforms the creation operator as $M_y c^\dagger_{l\alpha,k_y} = c^\dagger_{l\beta,-k_y}$, where α and β label the spin orientations and these spin indices should fulfil the condition that M_y conserves (flips) the y- (x- and z-) component spin[32,33]. When $\boldsymbol{d}_L$ and $\boldsymbol{d}_R$ are collinear with the z-axis, that is, $\theta_{L,R} = n\pi$ (n integer), the junction owns the M_y symmetry

$$M_y H(\phi, \theta_L, \theta_R) M_y^\dagger = H(\phi, \theta_L, \theta_R), \tag{11}$$

where $H(\phi, \theta_L, \theta_R)$ is the Hamiltonian described in Eq. 1 and ϕ is the superconducting phase difference. As the M_y transformation reverses the quantities: k_y and $s_{x,z}$, the M_y symmetry leads to the following relations

$$\begin{aligned} &\rho(l, k_y) = \rho\left(l, \bar{k}_y\right), s_x(l, k_y) = \bar{s}_x\left(l, \bar{k}_y\right) \\ &s_y(l, k_y) = s_y\left(l, \bar{k}_y\right), s_z(l, k_y) = \bar{s}_z\left(l, \bar{k}_y\right), \end{aligned} \tag{12}$$

where '$\bar{\cdot}$' denotes negative for compactness. Based on the current-density equations in Eq. 5 and Eq. 9, it follows that the $\pm k_y$ modes contribute oppositely and equally to i_y and j_y^z, respectively. Therefore, i_y is forbidden but j_y^z is allowed.

We can also perform another mirror transformation over the yz plane, which is denoted by the operator M_x. Under this transformation, one can obtain $M_x c^\dagger_{l\gamma,k_y} = c^\dagger_{-l\lambda,k_y}$. Here γ and λ are parallel (anti-parallel) when they denote the x- (y- and z-) component spins. When $\boldsymbol{d}_L$ and $\boldsymbol{d}_R$ are collinear, that is, $\theta_L = \theta_R + n\pi$, M_x transforms the junction as follows

$$M_x H(\phi, \theta_L, \theta_R) M_x^\dagger = H\left(\bar{\phi}, \theta_L, \theta_R\right). \tag{13}$$

Considering that the time-reversal symmetry exists in the junction except for an opposite ϕ

$$\mathcal{T} H\left(\bar{\phi}, \theta_L, \theta_R\right) \mathcal{T}^\dagger = H(\phi, \theta_L, \theta_R), \tag{14}$$

the junction has the *quasi*-M_x symmetry

$$\mathcal{T} M_x H(\phi, \theta_L, \theta_R) M_x^\dagger \mathcal{T}^\dagger = H(\phi, \theta_L, \theta_R), \tag{15}$$

where the '*quasi*' means the system possessing a M_x symmetry requiring a time-reversal transformation $\mathcal{T}$. For the M_x transformation changes the signs of l and $s_{y,z}$, and the $\mathcal{T}$ transformation reverses k_y and $s_{x,y,z}$[29], the *quasi*-M_x symmetry gives rise to

$$\begin{aligned} &\rho(l, k_y) = \rho\left(\bar{l}, \bar{k}_y\right), s_x(l, k_y) = \bar{s}_x\left(\bar{l}, \bar{k}_y\right) \\ &s_y(l, k_y) = s_y\left(\bar{l}, \bar{k}_y\right), s_z(l, k_y) = s_z\left(\bar{l}, \bar{k}_y\right). \end{aligned} \tag{16}$$

Through Eq. 5 and Eq. 9, it is under the *quasi*-M_x symmetry that both i_y and j_y^z are odd functions of l and their average values, I_y and J_y^z, are forbidden.

Then we consider the combined transformation of M_x and M_y, denoted by I_{xy}, which is actually the space inversion in the xy plane. When $\boldsymbol{d}_L$ and $\boldsymbol{d}_R$ are symmetric about the y- or z-axis, that is, $\theta_L + \theta_R = n\pi$, the junction possesses the *quasi*-I_{xy} symmetry

$$\mathcal{T} I_{xy} H(\phi, \theta_L, \theta_R) I_{xy}^\dagger \mathcal{T}^\dagger = H(\phi, \theta_L, \theta_R). \tag{17}$$

As the I_{xy} transformation alters the signs of l, k_y and $s_{x,y}$, and the $\mathcal{T}$ transformation reverses k_y and $s_{x,y,z}$, the *quasi*-I_{xy} symmetry results in

$$\begin{aligned} &\rho(l, k_y) = \rho\left(\bar{l}, k_y\right), s_x(l, k_y) = s_x\left(\bar{l}, k_y\right) \\ &s_y(l, k_y) = s_y\left(\bar{l}, k_y\right), s_z(l, k_y) = \bar{s}_z\left(\bar{l}, k_y\right). \end{aligned} \tag{18}$$

Again, based on Eq. 5 and Eq. 9, it is under the *quasi*-I_{xy} symmetry that i_y should be an even function of l while j_y^z the odd function. Therefore, J_y^z is forbidden but I_y is allowed.

The mirror symmetries can be seen clearly by plotting i_y and j_y^z versus l for several $\theta_{L,R}$, as shown in Fig. 2 and Fig. 3, respectively. As a result of the M_y symmetry, i_y is zero in the whole RSOC layer at ($\theta_L = 0, \theta_R = 0$). The *quasi*-$M_x$ symmetry is manifested by the anti-symmetric distribution of i_y at $(0.3\pi, 0.3\pi)$ and j_y^z at $(0, 0)$, $(0.3\pi, 0.3\pi)$. Due to the quasi-I_{xy} symmetry, i_y and j_y^z distribute symmetrically and anti-symmetrically at $(0.3\pi, -0.3\pi)$, respectively. At $(0.3\pi, 0)$, no symmetry holds and both I_y and J_y^z are non-zero. For the s-wave/RSOC/s-wave (s/RSOC/s) junction, those three symmetries, due to the isotropic s-wave pair potential, always hold and there is no i_y, I_y or J_y^z but j_y^z.

Apart from those special $\theta_{L,R}$, the mirror symmetries are broken and thus the transverse currents appear. However, the dependence of $I_y(\theta_{L,R})$ and $J_y^z(\theta_{L,R})$ on $\theta_{L,R}$

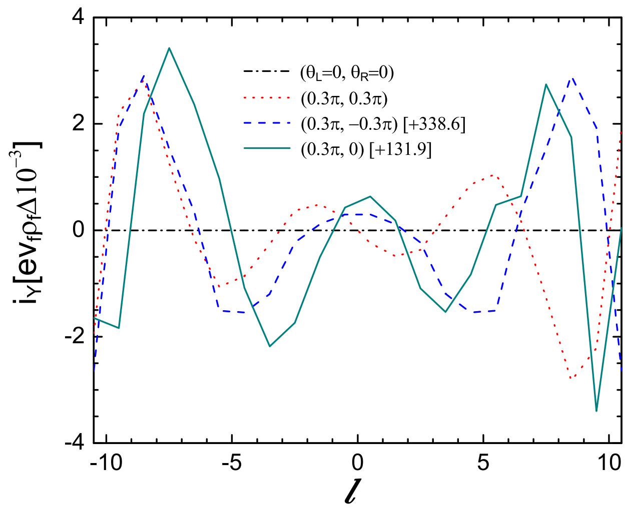

FIG. 2: Transverse charge current i_y versus column index l for several $\theta_{L,R}$ in the p_x/RSOC/p_x junction. Here $L = 20$, $T = 0.1T_c$, $\Delta = 0.01t$, $t_{so} = 0.05t$ and $\phi = 0.3\pi$. The line $\theta_L = 0.3\pi, \theta_R = -0.3\pi(0)$ is shift upward along the vertical axis by 338.6(131.9) units.

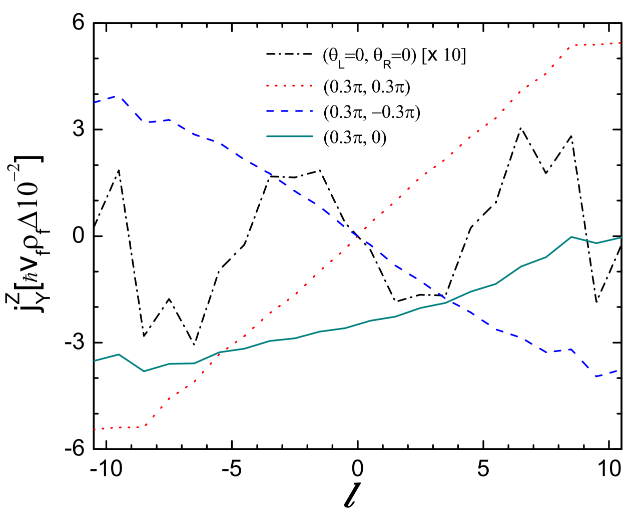

FIG. 3: Out-of-plane transverse spin current j_y^z versus column index l for several $\theta_{L,R}$ in the p_x/RSOC/p_x junction. Here $L = 20$, $T = 0.1T_c$, $\Delta = 0.01t$, $t_{so} = 0.05t$ and $\phi = 0.1\pi$. The line $(\theta_L = 0, \theta_R = 0)$ is multiplied by 10.

is strongly constrained by the mirror symmetries. It is easy to verify

$$\mathcal{T} M_x H\left[\phi, \theta_a, \theta_b\right] M_x^{\dagger} \mathcal{T}^{\dagger} = H\left[\phi, \theta_a, \bar{\theta}_b\right], \qquad (19)$$

where the Hamiltonian is reparameterized by the new angles $\theta_a = \left(\theta_L + \theta_R\right)/2$ and $\theta_b = \left(\theta_L - \theta_R\right)/2$. It shows that the junction with $[\theta_a, \theta_b]$ is the *quasi*-mirror image of the one with $\left[\theta_a, \bar{\theta}_b\right]$ and thus they should have opposite I_y and J_y^z. In other words, I_y and J_y^z are odd functions of θ_b. It is also found

$$\mathcal{T} I_{xy} H\left[\phi, \theta_a, \theta_b\right] I_{xy}^{\dagger} \mathcal{T}^{\dagger} = H\left[\phi, \bar{\theta}_a + n\pi, \theta_b\right], \qquad (20)$$

from which it follows that the two junctions with $[\theta_a, \theta_b]$ and $\left[\bar{\theta}_a + n\pi, \theta_b\right]$ should have the equal(opposite) $I_y(J_y^z)$, that is, $I_y(J_y^z)$ is symmetric (anti-symmetric) about $\theta_a = n\pi/2$.

IV. RESULTS AND DISCUSSION

In the numerical calculations, we only focus on the average transverse currents. As I_y and J_y^z originate from the broken mirror symmetries, care must be taken to avoid those special $\theta_{L,R}$ when plotting current-phase relations such as $I_y(\phi)$ and $J_y^z(\phi)$, as shown in Fig. 4. Here $L = 20$, $T = 0.1T_c$, $\Delta = 0.01t$, $t_{so} = 0.05t$, and $\theta_L = 0.3\pi$ are set. It shows that both I_y and J_y^z oscillate with ϕ with a period of 2π and vanish at $\theta_R = 0.3\pi = \theta_L$, where the junction has the *quasi*-M_x symmetry. These results are very different from the vanishing I_y and J_y^z in the s/RSOC/s junction[17], which possesses the M_y, *quasi*-M_x, and *quasi*-I_{xy} symmetries simultaneously. Therefore, the non-special orientation of $\boldsymbol{d}_{L,R}$ in the TS leads is a crucial ingredient to break the mirror symmetries and induce the transverse currents. Moreover, due to the constraint of the time-reversal symmetry[29], I_y and J_y^z are odd and even functions of ϕ, respectively.

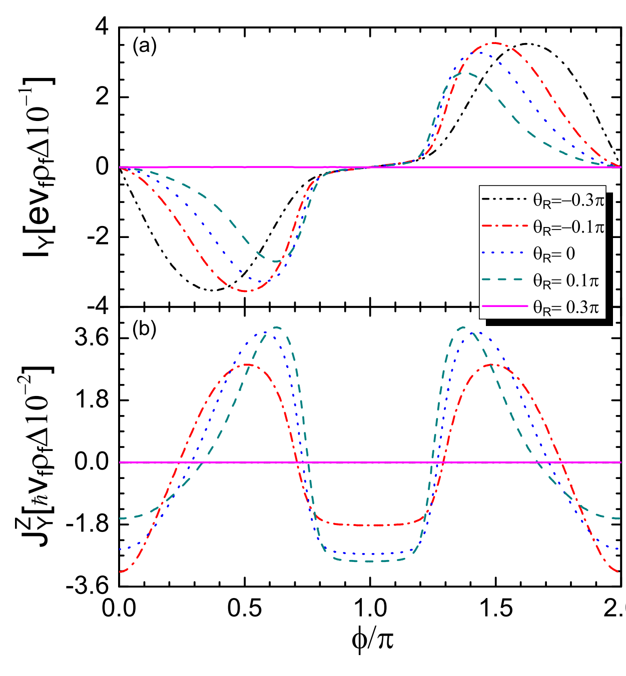

FIG. 4: The average transverse currents versus phase difference ϕ for several θ_R of the p_x/RSOC/p_x junction. (a) charge current I_y; (b) out-of-plane spin current J_y^z. Here $L = 20$, $T = 0.1T_c$, $\Delta = 0.01t$, $t_{so} = 0.05t$ and $\theta_L = 0.3\pi$.

Next we show the dependence of I_y and J_y^z on the orientation of $\boldsymbol{d}_{L,R}$, the RSOC strength, and the length of the RSOC layer. Due to the constraint of the *quasi*-M_x symmetry, both I_y and J_y^z are odd functions of θ_b, as shown in Fig. 5. Meanwhile, because of the constraint of the *quasi*-I_{xy} symmetry, I_y and J_y^z are respectively symmetric and anti-symmetric about $\theta_a = n\pi/2$, as shown in Fig. 6. Note that the nodal points of J_y^z at $\theta_a = n\pi/2$ in Fig. 6(b) are manifestations of the *quasi*-I_{xy} symmetry. As shown, the above numerical results are exactly consistent with the symmetry analysis in the last section.

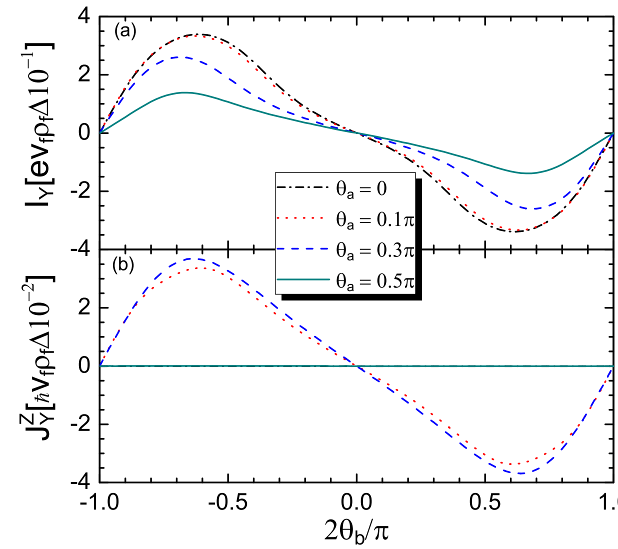

FIG. 5: The avarage transverse currents versus relative angle $\theta_b(2\theta_b)$ for several absolute angles θ_a of the p_x/RSOC/p_x junction. (a) I_y, $\phi = 0.3\pi$; (b) J_y^z, $\phi = 0.1\pi$. Here $L = 20$, $T = 0.1T_c$, $\Delta = 0.01t$ and $t_{so} = 0.05t$. $\theta_a(\theta_b) = (\theta_L \pm \theta_R)/2$.

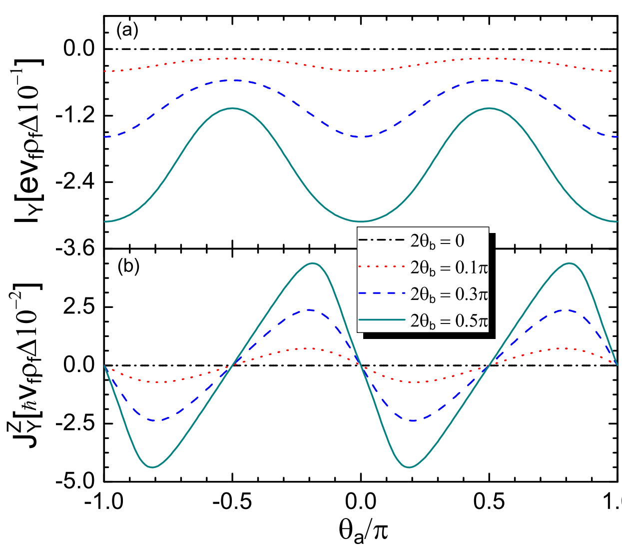

FIG. 6: The avarage transverse currents versus absolute angle θ_a for several relative angles θ_b of the p_x/RSOC/p_x junction. (a) I_y, $\phi = 0.3\pi$; (b) J_y^z, $\phi = 0.1\pi$. Here $L = 20$, $T = 0.1T_c$, $\Delta = 0.01t$ and $t_{so} = 0.05t$. $\theta_a(\theta_b) = (\theta_L \pm \theta_R)/2$.

In Fig. 7 and Fig. 8, we present I_y and J_y^z with the variations of the RSOC strength t_{so} and the length L of the RSOC layer, respectively. It is found that both I_y and

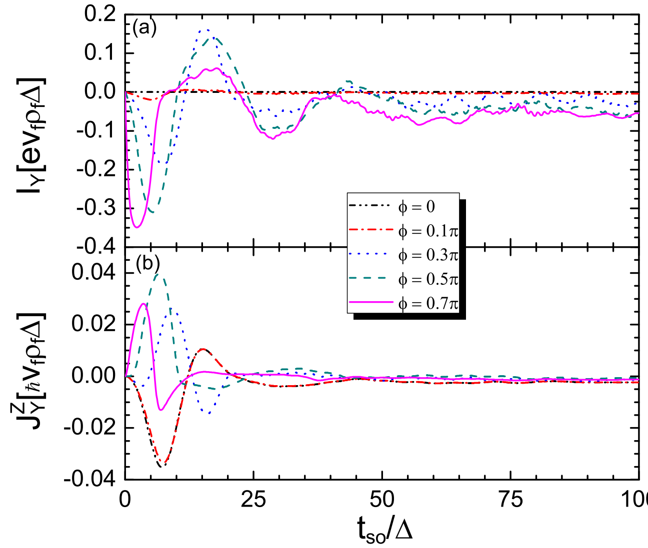

FIG. 7: The average transverse currents versus RSOC strength t_{so} for several phase differences ϕ of the p_x/RSOC/p_x junction. (a) I_y and (b) J_y^z. Here $L = 20$, $T = 0.1T_c$, $\Delta = 0.01t$, $\theta_L = 0.3\pi$ and $\theta_R = 0$.

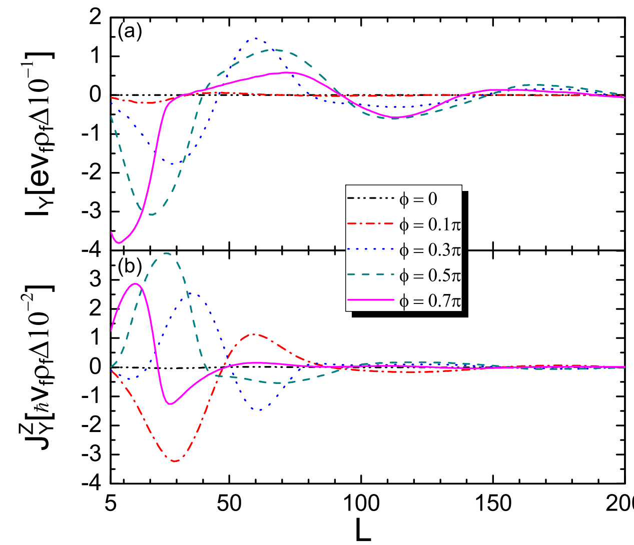

FIG. 8: The average transverse currents versus the length L of the RSOC layer for several phase differences ϕ of the p_x/RSOC/p_x junction. (a) I_y and (b) J_y^z. Here $T = 0.1T_c$, $\Delta = 0.01t$, $t_{so} = 0.05t$, $\theta_L = 0.3\pi$ and $\theta_R = 0$.

J_y^z oscillate and change their signs as t_{so} and L increase, and at larger t_{so} and L, the transverse currents tend to vanish. When t_{so} and L increase, the correlation between the two TS leads is weakened and the transverse currents decrease. Meanwhile, it is also seen that the directions of I_y and J_y^z can be reversed by either L or t_{so}, which is coming from the fact that TS Cooper pairs traveling in the RSOC layer obtain a spin precession phase[34] $t_{so} * La$. Therefore, the transverse currents should oscillate and damp with L or t_{so}.

Although we have focused on the TS/RSOC/TS junction with only p_x symmetry considered, our symmetry analysis is also applicable to other types of TS/RSOC/TS junctions with time reversal symmetry. One example is the p_y/RSOC/p_y junction, where both $\boldsymbol{d}_L$ and $\boldsymbol{d}_R$ are in the xz plane. The M_y symmetry is spontaneously conserved and thus i_y (also I_y) is forbidden. Meanwhile, the *quasi*-I_{xy} symmetry only holds at $\theta_{L,R} = n\pi$ where J_y^z is forbidden. Moreover, J_y^z is also forbidden at $\theta_L + \theta_R = n\pi$, where the junction owns the *quasi*-M_x symmetry. Another example is with $\boldsymbol{d}_{L,R} \sim k_x \boldsymbol{y} - k_y \boldsymbol{x}$, which possesses those three mirror symmetries simultaneously. Therefore, there is no i_y but the anti-symmetrically distributed j_y^z. These qualitative results are also numerically confirmed but not shown here. For $\boldsymbol{d}_{L,R} \sim (k_x + ik_y)\,\boldsymbol{z}$[20], the time-reversal symmetry is broken and the symmetry analysis above is invalid, but the numerical results show the anti-symmetrically distributed i_y and j_y^z. Moreover, through out this paper, the electric field affecting the RSOC, $t_{so}\,(\boldsymbol{k} \times \boldsymbol{\sigma}) \cdot \boldsymbol{e}$, is assumed normal to the xy plane and the electron motions are also confined in the xy plane. For other orientation of $\boldsymbol{e}$, our symmetry analysis is also applicable.

V. CONCLUSION

In summary, we have investigated the possible charge and spin Hall currents flowing in a p_x/RSOC/p_x hybrid junction. It is shown that the breaking of mirror symmetries of the junction due to some non-special orientations of two $\boldsymbol{d}$-vectors can induce transverse currents, which are sensitive to both the absolute and relative angles of the $\boldsymbol{d}$-vectors. Moreover, the symmetry analysis here is also applicable to other types of Josephson junction, such as the s/RSOC/s junction and TS/RSOC/TS junction with time-reversal symmetry. These findings shed new light on the equilibrium spintronic device design and are useful for identifying p-wave superconductor.

Acknowledgements

This work is supported by the General Research Fund of the Research Grands Concil of Hong Kong SAR, China (Project No. CityU100311/11P), Natural Science Foundation of China (Grant Nos. 110704032 & 11074233) and NSF of Jiangsu province (Grant No. BK2010416).

[*] Electronic address: apkschan@cityu.edu.hk
[†] Electronic address: zjlin@ustc.edu.cn

[1] E. H. Hall, Am. J. Math. **2**, 287 (1879).
[2] J. E. Hirsch, Phys. Rev. Lett. **83**, 1834 (1999).
[3] E. M. Hankiewicz, L. W. Molenkamp, T. Jungwirth and J. Sinova, Phys. Rev. B **70**, 241301 (2004).
[4] J. Wunderlich, B. Kaestner, J. Sinova and T. Jungwirth, Phys. Rev. Lett. **94**, 047204 (2005).
[5] S. O. Valenzuela and M. Tinkham, Nature **442**, 176 (2006).
[6] L. K. Werake, B. A. Ruzicka and H. Zhao, Phys. Rev. Lett. **106**, 107205 (2011).
[7] B. D. Josephson, Phys. Lett. **1**, 251 (1962).
[8] P. W. Anderson and J. M. Rowell, Phys. Rev. Lett. **10**, 230 (1963).
[9] V. V. Ryazanov, V. A. Oboznov, A. Yu. Rusanov, A. V. Veretennikov, A. A. Golubov and J. Aarts, Phys. Rev. Lett. **86**, 2427 (2001).
[10] T. Kontos, M. Aprili, J. Lesueur, F. Genêt, B. Stephanidis and R. Boursier, Phys. Rev Lett **89**, 137007 (2002).
[11] A. I. Buzdin, Rev. Mod. Phys. **77**, 935 (2005).
[12] A. A. Reynoso, G. Usaj, C. A. Balseiro, D. Feinberg and M. Avignon, Phys. Rev. Lett. **101**, 107001 (2008).
[13] A. Zazunov, R. Egger, T. Jonckheere and T. Martin, Phys. Rev. Lett. **103**, 147004 (2009).
[14] N. M. Chtchelkatchev and Yu. V. Nazarov, Phys. Rev. Lett. **90**, 226806 2003.
[15] B. Béri, J. H. Bardarson and C. W. J. Beenakker, Phys. Rev. B **77**, 045311 (2008).
[16] O. V. Dimitrova and M. V. Feigel'man, JETP **102** 652 (2006).
[17] A. G. Mal'shukov and C. S. Chu, Phys. Rev. B **78**, 104503 (2008).
[18] A. G. Mal'shukov, S. Sadjina and A. Brataas, Phys. Rev. B **81**, 060502 (2010).
[19] I. J. Lee, M. J. Naughton, G. M. Danner and P. M. Chaikin, Phys. Rev. Lett. **78**, 3555 (1997).
[20] A. P. Mackenzie, Y. Maeno, Rev. Mod. Phys. **75**, 657 (2003).
[21] Y. Asano, Y. Tanaka, M. Sigrist and S. Kashiwaya, Phys. Rev. B **67**, 184505 (2003).
[22] B. Kastening, D. K. Morr, D. Manske, and K. Bennemann, Phys. Rev. Lett. **96**, 047009 (2006).
[23] P. M. R. Brydon, C. Iniotakis, D. Manske, and M. Sigrist, Phys. Rev. Lett. **104**, 197001 (2010).
[24] Y. Asano, Phys. Rev. B **72**, 092508 (2005).
[25] P. M. R. Brydon, Y. Asano and C. Timm, Phys. Rev. B **83**, 180504 (2011).
[26] Y. Rahnavard, G. Rashedi and T. Yokoyama, J. Phys. Condens. Matter **23**, 275702 (2011).
[27] Z. H. Yang, J. Wang and K. S. Chan, J. Phys. Condens. Matter **23**, 085701 (2011).
[28] K. Sengupta and V. M. Yakovenko, Phys. Rev. Lett. **101**, 187003 (2008).
[29] Chi-Ken Lu and S. Yip, Phys. Rev. B **80**, 024504 (2009).
[30] M. Sigrist and K. Ueda, Rev. Mod. Phys. **63**, 239 (1991).
[31] P. A. Lee and D. S. Fisher, Phys. Rev. Lett. **47**, 882 (1981).
[32] B. K. Nikolić, L. P. Zârbo and S. Souma, arXiv:0907.4122v1[cond-mat.mes-hall].
[33] S. H. Chen, S. Maekawa, M. H. Liu and C. R. Chang, J. Phys. D: Appl. Phys. **43**, 015003 (2010).
[34] Z. H. Yang, J. Wang and K. S. Chan, J. Phys. Condens. Matter **22**, 045302 (2010).